Journal of Materials Chemistry A

Electronic Supplementary Information

Novel high-temperature supercapacitor combined dye sensitized solar cell from sulfated β-cyclodextrin/ PVP/MnCO$_3$ composite

S.Selvam[a], B. Balamuralitharan[a], S.N.Karthick[a], A. Dennyson Savariraj[a], K.V.Hemalatha[b], Soo-Kyoung Kim[a], Hee-Je Kim*[a],

[a]School of Electrical Engineering, Pusan National University, Gumjeong-Ku, Jangjeong-Dong, Busan 609-735, South Korea.

[b]Department of Chemistry, Coimbatore Institute of Technology, Coimbatore, Tamil Nadu, India.

E-mail: heeje@pusan.ac.kr;

sselvam222@gmail.com.

hemaac@gmail.com

1. Materials used

Poly-N-vinyl-2-pyrrolidone, N, N-dimethylformamide, sodium carbonate (Na$_2$CO$_3$), sulfuric acid (H$_2$SO$_4$), β-cyclodextrin, calcium carbonate (CaCO$_3$), acetic acid, potassium permanganate (KMnO$_4$) and poly(tetrafluorethylen), 1-butyl-3-methylimidazolium bis (trifluoromethylsulfonyl)imide [BMI][TFSI] were purchased from Sigma Aldrich. Ethanol was provided by Samchun chemicals.

2. Characterization techniques

XRD patterns were collected on a Powder X-ray diffraction of XPERT-PRO X-ray diffractometer with Cu-Kα anode radiation (λ=1.5418 Å) in the 2θ range of 10-90°and with a scan rate of 2°/min. The XPS spectra carried out by Theta Probe AR-XPS System (Thermo Fisher Scientific-U.K; X-ray source: monochromated Al Ka, hv=1486.6eV; X-ray energy: 15kv, 150W; Spot size: 400µm). Surface morphology of materials such as SEM analyzed by FE-SEM- Hitachi: S-4200 and TEM examined by JEOL TEM: JEM 2011 (Vac : 200 kV; CCD camera 4k x 4k -Ultra Scan 400SP). Thermo gravimetric analysis (TGA) graphs were verified on SDT Q600 V20 instrument in nitrogen atmosphere with a heating rate of 5°C/min. All the electrochemical analyses were done using BioLogic-SP150 workstation with three electrode setup. The DSSC current-voltage characteristics were studied under 1 sun illumination (AM 1.5G 100 mW cm^{-2}) using ABET Technologies solar stimulator with ±3% uniformity irradiance. The galvanic charge-discharge studies of supercapacitors were carried out in Arbind instrument (BT-2000).

3. FTIR analysis
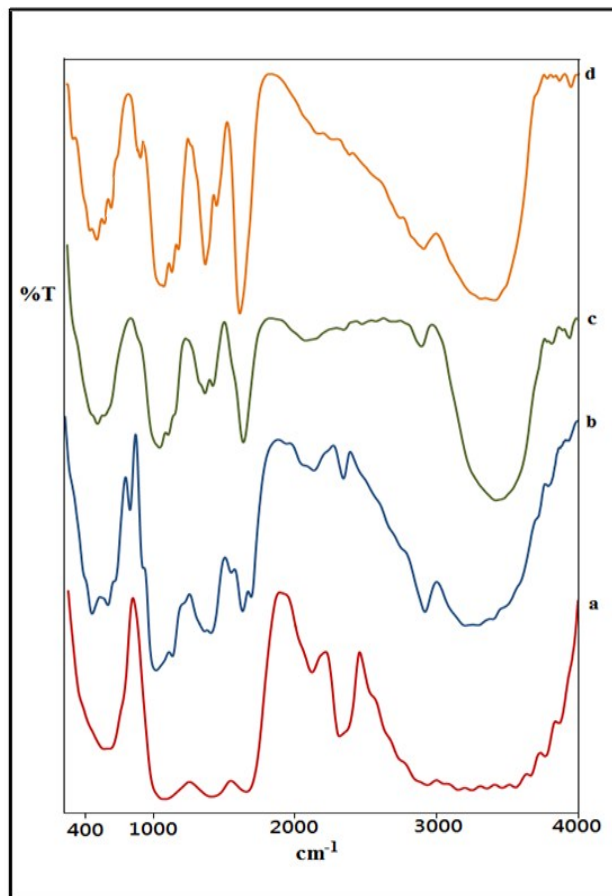
Fig. 1. FTIR analysis of β-CD (a), Sb-CD (b), PVP(c) and Sb-CD/PVP/MnCO$_3$(d) composites.

The FTIR spectra were measured by transmission mode using Perkin Elmer IR SPECTRUM ASCII PEDS 1.60 instrument with KBr pellets. The -OH stretching absorption displayed a typical broad peak from 3557 cm^{-1} to 3247 cm^{-1} (Fig. 1.4a). It indicates that the compound has many hydroxyl groups in β-cyclodextrin. The peak from 2932 cm^{-1} to 2119 cm^{-1} represented the -CH$_2$ groups. The stretching vibration of C-O-C bond has been identified at 1413 cm^{-1} and 1079 cm^{-1}. It is evidence for glucose linkages in β-cyclodextrin structure.

The Fig. 1.b expresses the FTIR spectrum of sulfated β-cyclodextrin (Sb-CD). A broad peak at 3207 cm^{-1} indicates the -OH stretching and this broad peak is smaller than β-cyclodextrin -OH broad peak. It exhibits the available free hydroxyl groups in Sb-CD. The peak values from 2924cm^{-1} to 2144 cm^{-1} exhibited the -CH$_2$ asymmetric stretching. The S-O stretching absorption peak is exhibited at 699 cm^{-1}. The asymmetric and symmetric stretching of -SO$_3$ groups from Sb-CD showed in the range from 1152 cm^{-1} to 699 cm^{-1}. It is the evidence that the sulfonic acid reacted on the β-cyclodextrin may involve sulfonation reaction. Fig 1. c shows a peak at 1654 cm^{-1} that is assigned to the stretching vibration of the C-O in PVP. The other important peaks at 1285 cm^{-1} and 1438 cm^{-1} are referring to the C-N stretching vibration and the attachment of -CH$_2$ groups in pyrrole ring of PVP. The FTIR spectrum of Sb-CD/PVP/MnCO$_3$ is exhibited reduction of broad hydroxyl absorption and evidence for hydroxyl group interaction with PVP by thermal crosslinking (Fig 1.d). A peak at 2906 cm^{-1} corresponds to -CH$_2$ stretching and the S-O stretching is the evidence represents at 1113 cm^{-1}. The stretching of C-N bond of PVP indicated by peaks at 1286 cm^{-1} and 1348 cm^{-1}. The characteristic peaks at 1448 cm^{-1} and 861 cm^{-1} were assigned to CO$_3^{2-}$ vibrations. [1] As a non-ionic surfactant, it was difficult for PVP to form strong chemical bond on the surface of the particles and PVP may be adsorbed on the surface through some weak force

2. EDX analysis
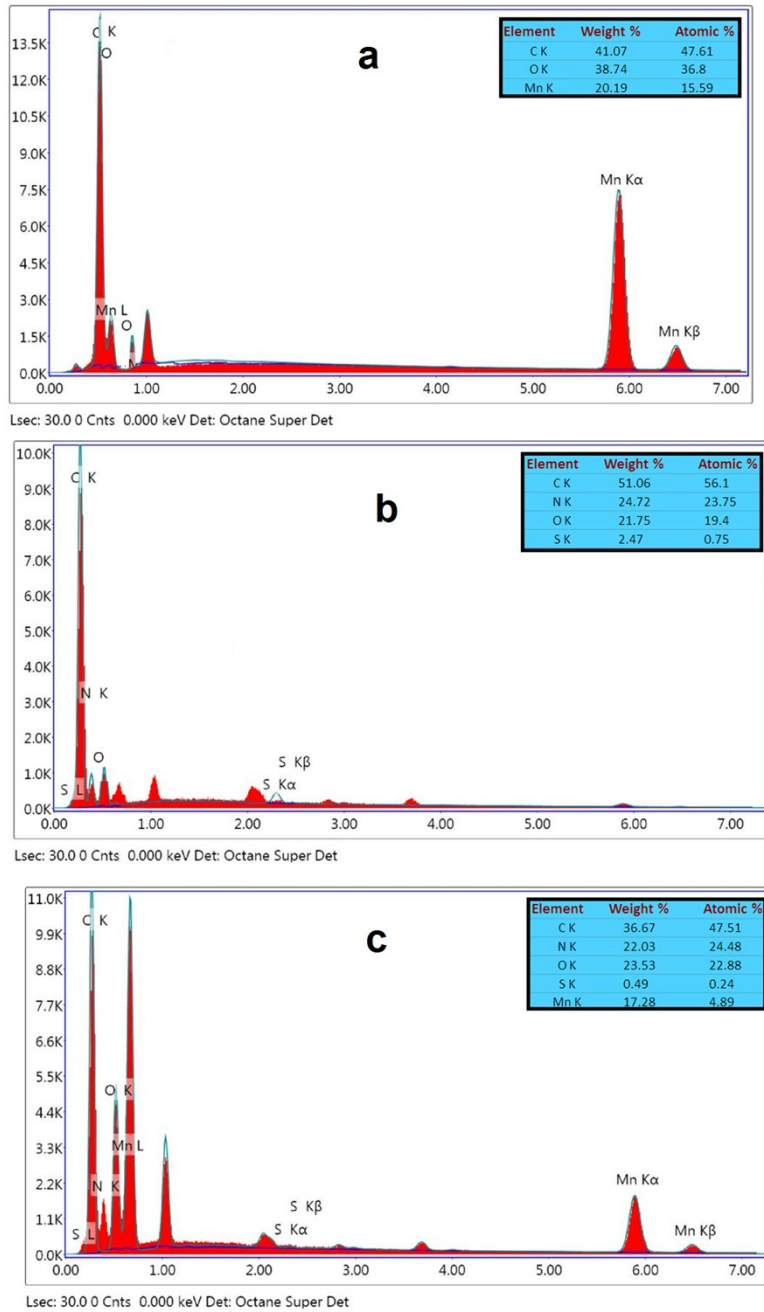
Fig 2. EDX analysis of MnCO₃ nanoparticles (a), Sb-CD/PVP(b) and Sb-CD/PVP/MnCO₃ composites

The EDX spectrum (2. a) shows the Mn, C & O elements and evidence for Mn is in the form of carbonate. Fig (2 .b) indicates Sulfur and Nitrogen present in Sb-CD modified polymer. This is the indication for Sb-CD crosslinked. In figure 2.c, the MnCO₃ nanoparticles showed on Sb-CD/PVP composite surfaces. Also other important S and N elements exhibited in EDX spectrum.

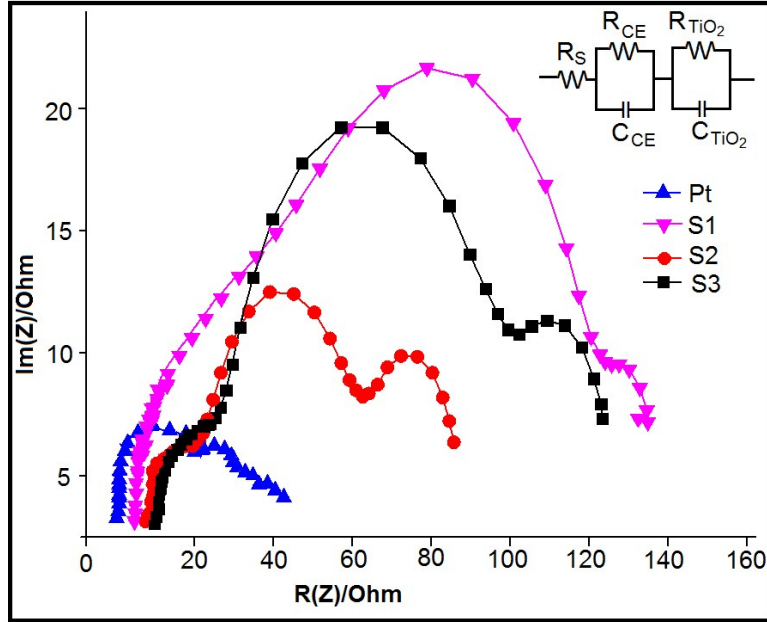**3. Electrochemical Impedance analysis of composite counter electrodes**

Fig. 3. Imbedance analysis of S1, S2 and S3 counter electrode DSSCs

Table1. Electrochemical impedance spectroscopy fitting results for Pt, S1, S2 and S3 Counter electrodes

Samples	$R_s(\Omega)$	$R_{CE}(\Omega)$	$R_{TiO_2}(\Omega)$
Pt	8.6	9.2	36.4
S1	8.9	20.7	86.5
S2	11.3	10.1	54.1
S3	16.1	20.3	73.6

Table 2. The calculated values of Rs, Cdl, Rct and Cp through fitting of the impedance spectra based upon the proposed equivalent circuit for supercapacitor

Parameters	Sb-Cd	Sb-CD/PVP	S1	S2	S3
$R_s(\Omega)$	5.8	5.4	4.9	5.0	4.8
$C_{dl}(F)$	$36.8e^{-6}$	$42.3e^{-6}$	$54.2e^{-6}$	$59.1e^{-6}$	$66.5e^{-6}$
$R_{ct}(\Omega)$	9.2	10.1	8.6	7.8	6.2
$C_p(F)$	$11.6 e^{-6}$	$7.3e^{-6}$	$6.2e^{-6}$	$5.7e^{-6}$	$4.3e^{-6}$

4. Jsc properties of composites

Fig. 3 showed the Jsc properties of composite CE. 6.5 J_{sc} resulted for Sb/cd composite and the J_{sc} increased with additon of $MnCO_3$ nanoparticles. The S2 composite DSSC show higher J_{sc} of 11.6 than S3, S1, and Sb/cd samples in ionic liquid electrolyte.
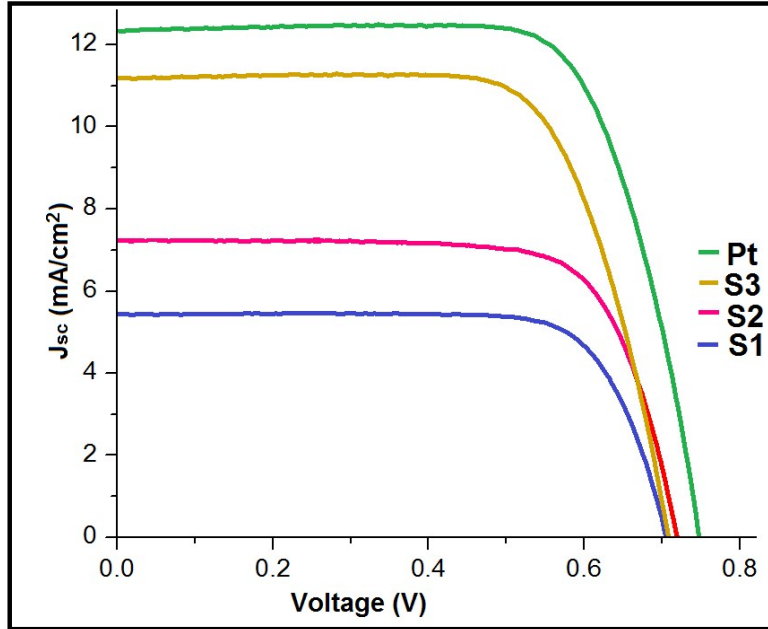

Fig. 4 J-V curves of DSSCs fabricated with Sb-CD, S1, S2, S3 composites
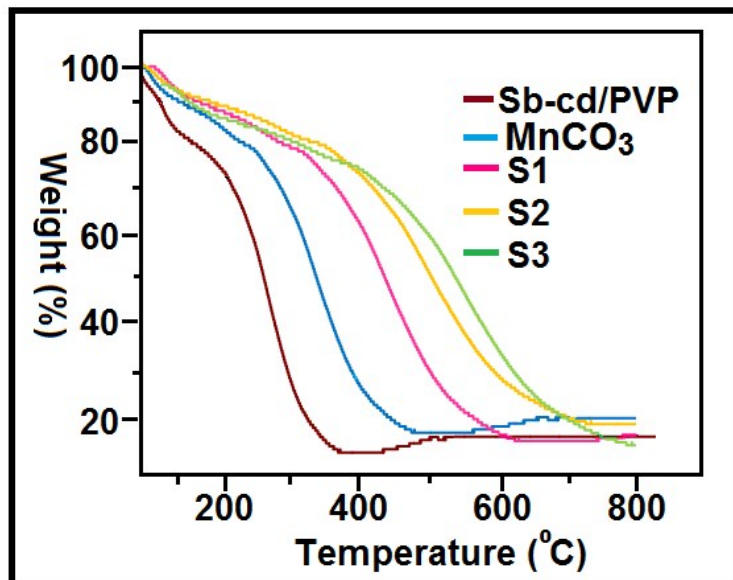
5. Thermal analysis

Fig. 5. TGA curve of Sb-CD/PVP, $MnCO_3$ and Sb-CD/PVP/$MnCO_3$ composites (S1, S2& S3)

The thermal stability performances of composite showed in figure 4. All the samples exhibits small weight loss of below 100˚C is assigned to the release of moisture from the electrodes. The Sb-CD/PVP composites show one-stage degradation within the range of 220-400˚C. The $MnCO_3$ nanoparticles under heating treatment exhibit a progressive weight loss shown in TG curve at 25-270ºC. It is indication of the removal of physically adsorbed water and much tightly bound water. A major weight loss is exhibit at temperature range from 200ºC to 410ºC, which is due to the release of CO_2 by the decomposition of $MnCO_3$. In Sb-CD/PVP/$MnCO_3$ composite the mass loss at 410ºC to 630ºC temperature stage matches well with theoretical analysis of mass loss when $MnCO_3$ decomposed to MnO_2. This also provides evidence for the formation of MnO_2 as intermediate product. The slight weight loss at temperatures higher than 400ºC could be attributed to the discharge of oxygen during the conversion from $MnCO_3$ to MnO_2 and Mn_2O_3. The reaction rapidity was enhanced when the temperature is higher than 490ºC. The total mass loss during this passé from 400ºC to 650ºC is a little bit smaller than the theoretical prediction. The weight loss difference is hard to detect at temperatures above 620ºC. This may indicate the formation of pure phase Mn_2O_3.[2] These processes can be described as the following equations 1&2.

$$2MnCO_3 + CO_2 \rightarrow 2MnO_2 + CO_2 \ .....1$$

$$4MnO_2 \rightarrow 2Mn_3CO_3 + O_2 \ ....2$$
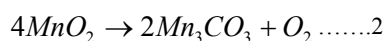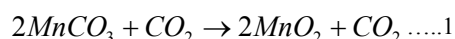
The Sb-CD/PVP composites are also showing relatively high thermal stability due to strong intra- and inter-molecular hydrogen bonds. From these results the thermal stability of prepared composite electrodes is high and suitable for heat environment devices.

6. Calculations

Capacitance could also be calculated from the galvanostatic discharge curves, using the following equation 3.

$$C = \frac{I\Delta t}{m\Delta V} \ .....3$$

Where I (A) is charge or discharge current, Δt (s) is the time for a full charge or discharge, m (g) indicates the mass of the active material, and ΔV represents the voltage change after a full charge or discharge.

The energy density (E) calculated by equation 4 and power density (P) were calculated by equation 5.

$$E = \frac{C(\Delta V)^2}{2} \ .....4$$

$$P = \frac{E}{\Delta t} \ ......5$$

Where C is the specific capacitance of the active materials, and ΔV is the potential window of discharge.

References

1. L.X.Yang, Y.Liang, H.Chen, Y.F.Meng, W.J. Mater Res Bull, 2009, 44, 1753-1759

2. X.Wang, S.Qiu, G.Lu, C.He, J.Liu, L.Luan and W.Liu. CrystEngComm, 2014, 16, 1802-1809.